Available online at www.sciencedirect.com
SCIENCE DIRECT®
Talanta 65 (2005) 1132–1142
Talanta
www.elsevier.com/locate/talanta

Sensor applications of attenuated total reflection infrared spectroscopy

C. Vigano, Jean-Marie Ruysschaert, Erik Goormaghtigh*

Laboratory for the Structure and Function of Biological Membranes, Center for Structural Biology and Bioinformatics, Free University of Brussels, Campus Plaine CP206/2, 1050 Brussels, Belgium

Received 12 December 2003; received in revised form 27 May 2004; accepted 14 July 2004
Available online 23 November 2004

Abstract

Attenuated total reflection Fourier transform infrared spectroscopy is one of the most powerful methods for recording infrared spectra of biological materials in general, and of biological membranes in particular. It is fast, yields a strong signal with only a few micrograms of sample and recent ATR devices allow the recording of nanogram quantities. Importantly, it allows information about the orientation of various parts of the molecules under study to be evaluated in an oriented system. While mid-infrared radiation has been most used for fundamental research on molecular structure, it is becoming an interesting alternative for sensor research. In addition to the usual sensor response, one of its advantages is its sensitivity to molecular conformation. In turn, the binding of a drug onto a receptor may be monitored as for other detection methods but in addition the evaluation of the structural response of the receptor to this binding is likely to bring invaluable information on the mechanism of action of the drug. The present review focuses only on the ATR-mid IR spectroscopy with a special interest for proteins and biological membranes.

Keywords: Attenuated total reflection infrared spectroscopy; Membrane; Protein

1. Introduction

Attenuated total reflection Fourier transform infrared spectroscopy (ATR-FTIR) is one of the most powerful methods for recording infrared spectra of biological materials in general, and of biological membranes in particular. It is fast, yields a strong signal with only a few micrograms of sample, and most importantly, it allows information about the orientation of various parts of the molecules under study to be evaluated in an oriented system [1]. While mid-infrared radiation has been most used for fundamental research on molecular structure, it is becoming an interesting alternative for sensor research. In addition to the usual sensor response, one of its advantage is precisely its sensitivity to molecular conformation [2–5]. Protein conformation is also easily investigated [6–10] and may be of major interest for the understanding of the action of drugs on their protein receptors. For instance, the binding of a drug onto a receptor may be monitored as with other detection methods but in addition the evaluation of the structural response of the receptor to this binding is likely to bring invaluable information on the mechanism of action of the drug. Another interesting feature of the IR detection is that it allows the concentrations to be determined from the molar integrated extinction coefficients.

One major challenge when using mid-IR radiation is the strong absorbance of water. To some extent, the ATR technique alleviates the problem as the sensor is built on a very thin layer that is sensed by the evanescent field while the bulk of the solvent is not. Another challenge is the binding of the receptor molecules of interest to the internal reflection element (IRE). It must maintain the integrity of the protein structure and activity, and the modified surface must not present non-specific binding sites for the potential ligands.

Abbreviations: ATR, attenuated total reflection; AU, absorbance units; FTIR, Fourier transform infrared; IRE, internal reflection element; KRS-5, thallium iodide and chloride; MCT, mercury cadmium telluride

* Corresponding author. Tel.: +32 26505386; fax: +32 26505113.
E-mail address: egoor@ulb.ac.be (E. Goormaghtigh).

0039-9140/$ – see front matter © 2004 Elsevier B.V. All rights reserved.
doi:10.1016/j.talanta.2004.07.052

The present review focuses only on the ATR-mid IR spectroscopy with a special interest for proteins and biological membranes.

2. General principles

It is essential to understand the basic rules that govern the absorption of the IR light at the reflecting interface of the IRE. They have a profound impact on (1) the spectrum intensity, (2) the band shape, (3) the intensity ratio between bands located at different wavelengths, (4) the ratio between the contributions of the bulk of the solvent and the sample, (5) the quantitative evaluation of surface concentrations, (6) the impact of polymer or metallic layers on the signal-to-noise ratio. The reader is referred to Harrick and Fringeli [5,11] and to our recent review on ATR-FTIR applied to the study of biological membranes and proteins [1] for more details.

Various experimental set-ups of attenuated total reflection spectroscopy have been designed, including fiber optics for the study of proteins [12–15]. However, the most usual design is still the trapezoidal plate. A schematic representation of an ATR set-up appears in Fig. 1. The infrared beam is directed into a high refractive index medium which is transparent for the IR radiation of interest. Above a critical angle θ_c which depends on the refractive index of the internal reflection element (IRE), n_1, and of external medium, n_2,

$$\theta_c = \sin^{-1} n_{21} \tag{1}$$

($n_{21} = n_2/n_1$) the light beam is completely reflected when it impinges on the surface of the IRE. Several internal total reflections occur within the IRE until the beam reaches the end. It can be shown from Maxwell's equations that superimposition of incoming and reflected waves yields a standing wave within the IRE established normal to the totally reflecting surface. Importantly, an electromagnetic disturbance

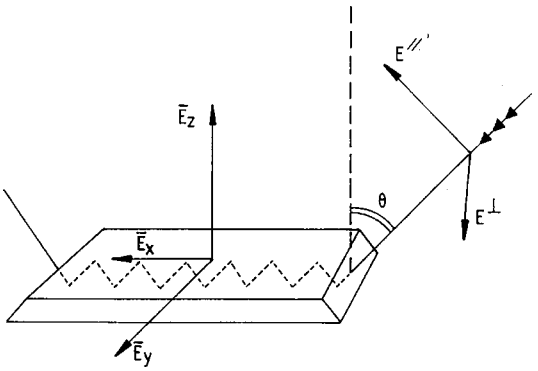

Fig. 1. Schematic representation of the a internal reflection element (IRE) and of the light pathway. The Cartesian components of the electric field are shown along the *X*, *Y* and *Z* axes. Two possible planes of polarization of the incident light are indicated by *E*// (polarization parallel to the incidence plane) and *E* ⊥ (polarization perpendicular to the incidence plane). The incident beam makes an angle *(* with respect to a normal to the IRE surface. The edges of the IRE are bevelled so that the incident beam penetrates the IRE through a surface that is perpendicular to its propagation.

also exists in the rarer medium beyond the reflecting interface. This so-called evanescent wave is characterized by its amplitude which falls exponentially with the distance from the interface according to

$$E = E_0 e^{-z/d_p} \tag{2}$$

where E_0 is the time averaged electric field intensity at the interface, E is the time averaged field intensity at a distance z from the interface in the rarer medium and d_p is the penetration depth of the evanescent field. It is given by

$$d_p = \frac{\lambda 1}{2\pi(\sin^2\theta - n_{21}^2)^{1/2}} \tag{3}$$

where $\lambda_1 = \lambda/n_1$ and $n_{21} = n_2/n_1$ [11]. The larger λ (or the smaller θ), the larger the penetration depth. Fig. 2 illustrates a typical decay of the evanescent field intensity on the μm range for total reflection in two different IREs. It is the presence of the evanescent field which makes possible the interaction between infrared light and the sample present on the surface of the IRE, within approximately the penetration depth of the field. An obvious conclusion that can be drawn is that the sample has to be in close contact with the IRE. Furthermore, the molecules from the bulk of the solvent are usually not sensed at all because they are too diluted and too far away from the reflecting interface. It is also apparent from Eq. (3) that band intensity will depend on the wavelength since the penetration depth, and thereby the interaction with the sample, increases with λ.

The principles described above yield spectral features which are specific to ATR spectroscopy. Two typical situations can be encountered.

2.1. The case of thick films

The absorbance depends on the square of the dot product $\left|\overline{E}(\partial\overline{\mu}/\partial q)\right|^2$ where μ is the transition dipole, q a normal coordinate and E is the electric field amplitude in the rarer medium. E is a function of z as described by Eq. (2). For any transition, it can be shown [11] that the absorbance is proportional to the so-called effective penetration depth defined as

$$d_e = \frac{n_{21}}{\cos\theta}\int_0^\infty E^2 dz = \frac{n_{21}E_0^2 d_p}{2\cos\theta} \tag{4}$$

where E is given by Eq. (2) and d_p by Eq. (3). The reader is referred to Harrick [11] for the derivation of the expression of the electric field amplitude. Eq. (4) indicates that:

- the effective depth of penetration is proportional to the wavelength through d_p. In turn, the absorbance is higher on the long wavelength side of the spectrum. The ratio between the intensity of two peaks is therefore different from the ratio obtained by transmission spectroscopy by a quite significant factor. As an example, the efficient thicknesses are 0.70 μm and 4.84 μm, respectively for germanium and KRS-5 IREs with the same geometry and a sam-

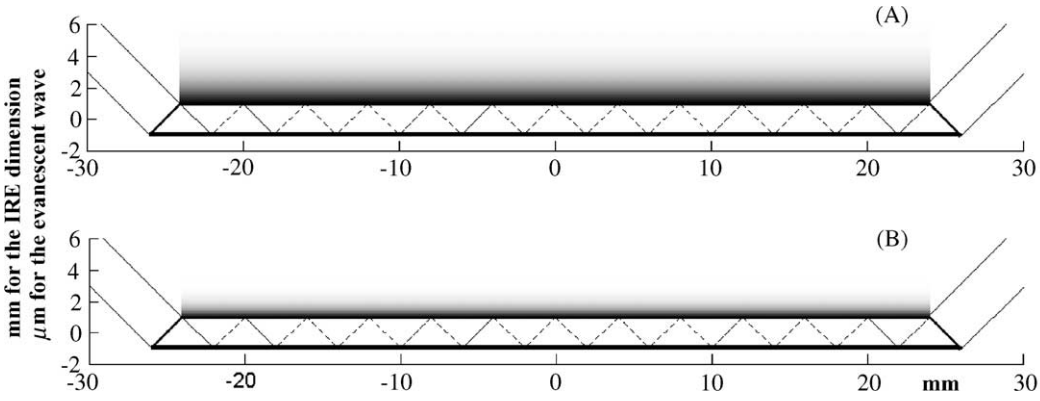

Fig. 2. Schematic representation of the evanescent wave on a 52 mm × 2 mm (A) KRS-5 and (B) germanium IRE, at 45° incidence, for a beam width of 3 mm. The grey density decreases as the intensity of the evanescent field. For the clarity, the evanescent field if represented only on the upper side of the IRE.

ple refractive index $n_2 = 1.44$ at 1650 cm^{-1} (Fig. 2). For a thick sample, spectra will be about seven-fold more intense for the KRS-5 IRE. Before selecting KRS-5 or other materials with lower refractive indices (see Table 1), the user must consider that the proximity of the critical angle will be responsible for spectrum distortions with respect to transmission spectra because of the marked influence of the refractive index variation in the absorbance bands [1]. Keeping away from θ_c is the safe way to obtain spectra closely resembling their transmission counterparts. In addition, using KRS-5 is certainly a bad choice if the additional penetration depth results only in an increase of the buffer contribution to the spectrum;

- another important consequence of this is that band shape is distorted in thick film ATR spectra, with more absorbance on the long wavelength band side and less absorbance on the short wavelength band side.

2.2. The case of thin films

In the case of a thin film, it is supposed that the film is thin enough so that there is no significant change of the electric amplitude in the evanescent wave over the film thickness. Therefore, if the film thickness d is small with respect to the wavelength, Eq. (4) becomes

$$d_e = \frac{n_{21}}{\cos\theta}\int_0^d E^2 dz = \frac{n_{21}E_0^2}{\cos\theta} \times \left(-\frac{d_p}{2}\right)(e^{-2d/d_p} - 1) \approx \frac{n_{21}E_0^2 d}{\cos\theta} \quad (5)$$

In this case,

- the effective thickness does not depend on the wavelength. In turn, band relative intensity is not distorted and

Table 1
Optical and physical properties of different IRE materials

Materials	n_1	θ_c (°) in water	Hardness (kg/mm^2)	Wavelength range	Comments	θ (°)	d_e (μm)	d_p (μm)
Ge	4.0	22	780	4000–830	Stable in water, in acids and alkalis attacked by hot H_2SO_4	30	1.92	0.73
						45	0.74	0.40
						60	0.39	0.31
Si	3.4	26	1150	4000–1500	Stable in water, in acids and alkalis attacked by HF and HNO_3	30	4.32	1.17
						45	1.17	0.51
						60	0.59	0.38
ZnSe	2.4	39	120	4000–650	Stable in water pH 5–9	45	5.29	1.22
						60	1.86	0.67
KRS-5	2.4	39	40	4000–400	Not very stable in water	45	5.29	1.22
						60	1.86	0.67
Diamond	2.35	40	Very hard	4000–400	Stable in water pH 1–14	45	6.17	1.35
						60	2.03	1.69
ZnS	2.2	43	355	4000–950	Stable in water, not at acidic pH	45	12.65	2.34
						60	2.75	0.82

Other materials such as CdTe ($n_1 = 2.65$, hardness = 45) are close to those described in the table. The values of the efficient penetration depth of the evanescent wave have been calculated at a wavelength of 1650 cm^{-1} for a randomly polarized light. The critical angle is calculated in water ($n = 1.5$). KRS-5 is a thallium bromide/thallium iodide eutectic.

absorption bands are no more broader on the long wavelength side. Therefore, spectra of thin films closely resemble their transmission counterparts;
- in the case of thin films, the effective thickness is proportional to d;
- d_e can be less or much greater than the actual film thickness, i.e. the absorbance is, in some conditions, much larger than the absorbance of the same film measured by transmission spectroscopy.

3. Considerations on multiple reflections

Until now, we examined the case of a single internal reflection. For a single reflection with low absorption, the reflectivity R is given by

$$R = 1 - \alpha d_e \tag{6}$$

where the absorption extinction coefficient α and d_e is the effective penetration depth or the effective thickness of the film, i.e. the thickness of the film which would yield the same absorption by transmittance. For N multiple reflections, the reflectivity is given by

$$R = (1 - \alpha d_e)^N \approx 1 - N\alpha d_e \tag{7}$$

when $\alpha d_e \ll 1$, i.e., the measured "absorbance" will be roughly N times the absorbance due to a single reflection. In turns, the geometric characteristics of the IRE strongly modulate the spectrum intensity. The parameters which must be considered are the length l and thickness t of the IRE, the incidence angle θ and the refractive index n_1. The number N of internal reflections is proportional to l and inversely proportional to t. It also increases as θ decreases according to

$$N = \frac{l}{t} \cot\theta \tag{8}$$

In turn, l, θ and t must be adjusted so that N is an integer and odd for the geometry described in Fig. 1. Counteracting the sensitivity increase at small incidence angles, the aperture A decreases, letting less light into the IRE

$$A = t\cos\theta \tag{9}$$

$$A = 2t\ \sin\theta \quad \text{for}\ \theta < 45^\circ \tag{10}$$

Highly sensitive MCT detectors available can overcome this problem to a certain extent

Fig. 3 demonstrates how the IRE thickness changes the number of reflections. For the 1 mm thick IRE, almost the entire area (94%) is sampled and 51 internal reflections occurs (25 on the upper surface and 26 on the lower surface in Fig. 3). On the other hand, when an 2 mm thick IRE is used, only 45% of the area is sampled and only 25 internal reflections occur. It turns out that sensitivity can be increased by choosing the appropriate IRE geometry.

The penetration depth of the evanescent wave increases as θ decreases as described by Eq. (3). When the index matching is better between the sample and the IRE (n_{21} close to 1 but not larger than $\sin\theta$), the penetration depth of the evanescent wave increases (see Eq. (3)). Furthermore, the relative importance of the layers close to the IRE surface can be modulated via the penetration depth. If a monomolecular film is to be studied in an aqueous environment, the contribution of the buffer with respect to this of the bilayer can be reduced by reducing the penetration depth (e.g. Fig. 2). If thick samples must be studied, this penetration depth can be larger. There are of course limits to both the incidence angle and n_1 value placed by the critical angle below which total reflection is lost (Eq. (1)).

Fig. 4 demonstrates the importance of setting a correct geometry for the IRE. In Fig. 4a and b, the IRE is the same but the incidence IR beam was open at 2 mm in Fig. 4a and 3 mm in Fig. 4b. It can be observed that for some incidence angles a fraction of the beam is not reflected at a position that allows it to quit the IRE (B panels). The film length sampled by the beam decreases with the incidence angle (C panels) as does the number of internal reflections (E panels) and the penetration depth (D panels). As the beam gets

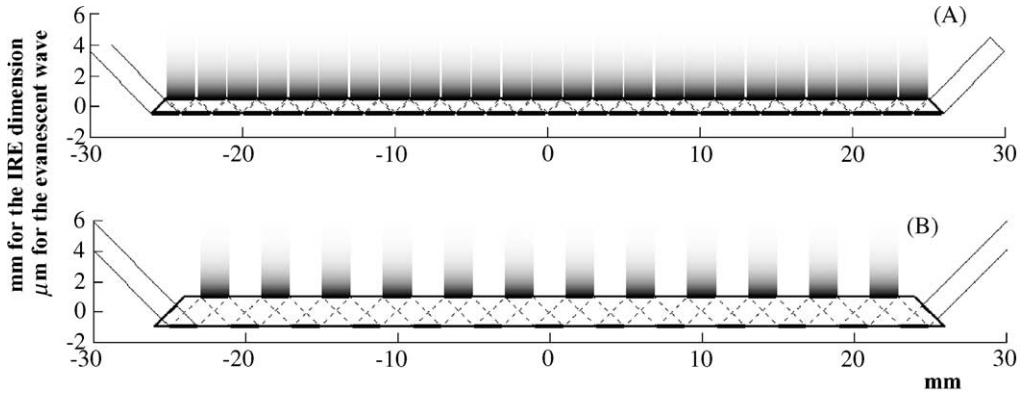

Fig. 3. Schematic representation of the evanescent wave on KRS-5 IRE on a 52 mm × 1 mm and (B) 52 mm × 2 mm plate, at 45° incidence, for a beam width of 1.3 mm. The grey density decreases as the intensity of the evanescent field. For the clarity, the evanescent field if represented only on the upper side of the IRE.

wider, only a fraction of it is able to penetrate into the IRE (A panels).

From the practical point of view, an important property of the IRE is its hardness (Table 1). Indeed, it determines how quickly the surface is going to be damaged. Since scattering follows a law in λ^{-4}, intensity losses at high wavenumbers quickly become considerable.

4. Sensor building

One of the challenges encountered in the design of FTIR-ATR-based sensors is the preparation of non-denaturating matrices for the immobilization of enzymes or even cells. The surface prepared should also prevent non-specific binding. Several ways of surface modification have been investigated.

4.1. Physical adhesion

Among the different sample used to coat the IREs, biological membranes are among the most important. They are usually difficult to handle, bear numerous proteins (20–30% of the genome codes for membrane proteins) and are privileged targets for drug research. The stability of physisorbed membranes onto an IRE in an aqueous environment have made this system attractive for the study of the partition of molecules between the water phase and the membrane since the eighties for investigations on peptides [16] or drugs [17].

4.2. Preparation of film by Langmuir–Blodgett transfer

The Langmuir–Blodgett technique allows the structure of a molecular assemblies of known structure to be maintained for the infrared investigation. The assembly on the IRE is obtained by transferring a monolayer spread at the air–water interface by a cycle of dipping and withdrawal of the IRE through the monolayer. The surface pressure of the monolayer is kept constant during the process by moving a barrier on the surface. The barrier displacement allows to control the amount of material transferred on the plate. The details of the technique are described elsewhere [18,19]. This procedure allows the study of single mono- or bilayer or multilayers arrangements with a thoroughly covered surface. The quality of coverage was found to depend on the head groups of the first monolayer, with better results reported for phosphatidylethanolamine [20,21]. Practically speaking, only single monolayers are easily obtained when working with phospholipids. Single monolayers of DPPC transferred on a germanium IRE at low pressure (20 mN/m) or high pressure (40 mN/m) results, respectively in ordered and disordered

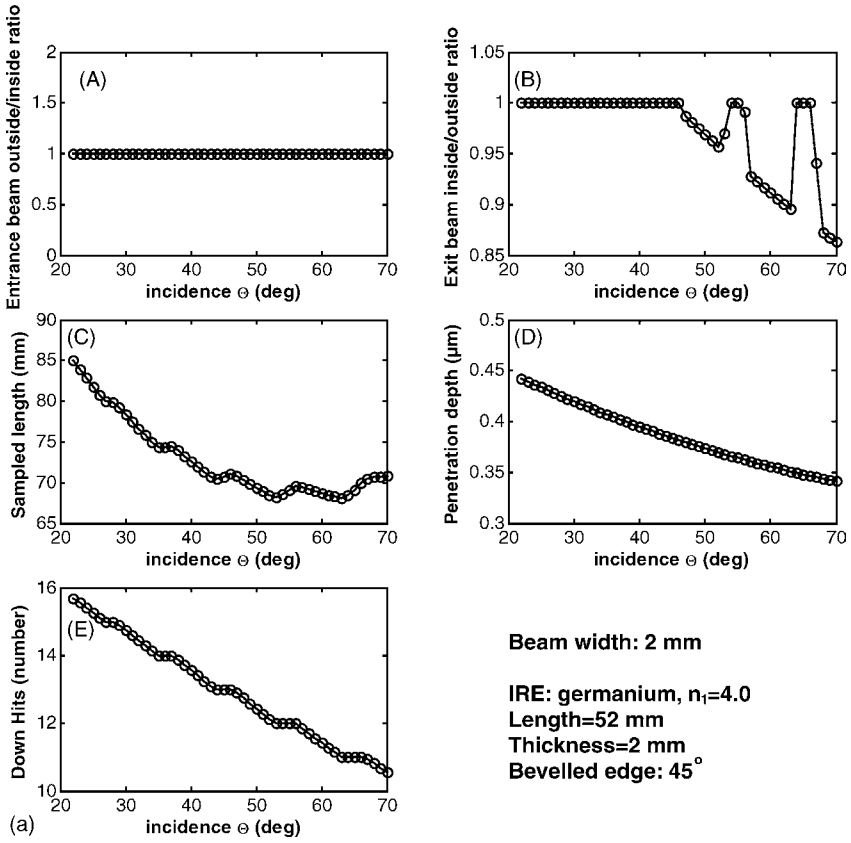

Fig. 4. (a) Evolution as a function of the incidence angle (beam width 2 mm) on a germanium IRE of: the fraction of the beam that really enter the IRE (A), the fraction of the beam present inside that can quit the IRE (B), the sampled length (C), the penetration depth d_p (D) and the number of reflections on the lower surface (see Figs. 2 and 3) (E). (b) As for (A) but for a 3 mm beam width.

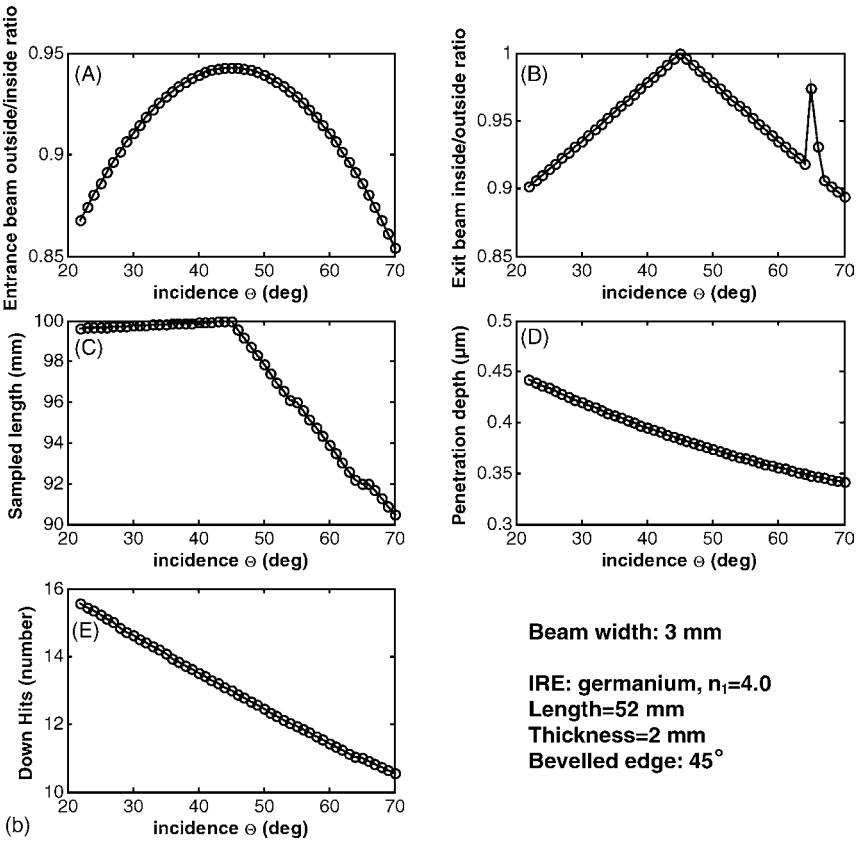

Fig. 4. (b) (*Continued*).

states of the DPPC molecules similar to those observed in liposomes below and above the phase transition. However, when the number of layers transferred (z-type) is increased, the ordered form is always found suggesting a rearrangement of the layers so that a closer packing of the molecules is obtained. Similar rearrangements of the DPPC molecules to form islands of well-packed molecules in monolayers transferred at low pressure have been suggested by Okamura et al. [22]. Other evidences of reorganization have been brought by Fringeli et al. [23,24]. A recent attempt to map out the potential artifacts of the film transfer [25] showed that the speed of transfer has an effect on the final structure. At fast transfer speed, the structure of the film molecules remains essentially unchanged. At slower speeds, reorganization of the film molecules occurred. Some practical aspects of the study of monolayers by IR have been reviewed recently [26,27]. This system has been extensively used for the study of the interaction of protein signal peptides with monolayer [28–30]. Pure peptidic monolayer have also been transferred successfully [31]

4.3. Adsorption from bulk phase method on Langmuir–Blodgett films

Because the Langmuir Blodgett method is very efficient to deposit a monolayer on the IRE but usually fails to deposit a second monolayer in order to form a phospholipid bilayer, the Langmuir–Blodgett technique is not suitable for the study of most integral membrane proteins. Fringeli (1989a) indicated an elegant method to overcome this limitation. In a first step, a monolayer is transferred on the IRE by the Langmuir–Blodgett technique. During withdrawal of the plate at ca. 1 cm/min, surface pressure is kept constant (40 mN/m). A monolayer is now present with the polar head groups of the lipids facing the IRE and the hydrophobic hydrocarbon chains facing the surrounding medium. In a second step, the monolayer-coated IRE is mounted in a liquid cell which is flowed with a vesicle suspension at ca 1 mg/ml. Spontaneous adsorption occurs on the hydrophobic monolayer and a bilayer is formed. Depending on the nature of the adsorbed second layer, the bilayer can be symmetric or asymmetric. The system designed by Fringeli et al. [32] is very attractive because it allows to monitor spectroscopically the adsorption of any water soluble molecule present in the buffer, to quantify its amount and to analyze its structure and orientation with respect to the lipid bilayer. It must be noted that while the first monolayer was made out of DPPA in the original work of Fringeli, POPC was found to be as efficient by Tamm and co-workers [33,34]. The experiment has been repeated in our laboratory (unpublished data) and was shown to quantitatively yield a monolayer of DPPA and a bilayer after incubation with POPC. The final assembly was stable over a period of several hours.

Insight into the mechanism of the deposition of the second layer can be obtained using deuterated lipids. If the second layer fuses with the existing layer, part of the ν(C–H) band intensities will be replaced by ν(C–D). If the second layer is adsorbed on top of the first one, intensity of the ν(C–H) will not decrease but the ν(C–D) bands will appear superimposed to the original spectrum.

The adsorption of a second bilayer on top of the first one is possible in some conditions. Fringeli et al. [32] demonstrated that membrane fragments enriched in Na^+, K^+-ATPase isolated from rabbit kidney adsorb spontaneously to a DPPA/POPC (POPC outside) bilayer. Even though firmly adsorbed, these vesicles seem to remain essentially intact and do not form a continuous bilayer.

4.4. Membrane multilayer stacks

Recently, it was found that in a number of situations lipid films prepared by solvent evaporation (either organic or aqueous in the case of natural membranes) can be immersed in bulk water without loss of materials. Originally, Ge IRE were cleaned by immersion in concentrated chromic acid for 30 min. Such a treatment on germanium crystals yields a surface on which purple membranes stick tightly for hours in the presence of an aqueous environment, provided that a high salt concentration is maintained [35]. Similar results were obtained for the nicotinic acetylcholine receptor by Baenzinger and co-workers [36–41]. It was shown later that the chromic acid treatment is not always necessary. In our laboratory, Ge IRE are cleaned first with a basic lab detergent (pH 11), then rinsed with distilled water and placed in a methanol-containing vessel. The IRE is then transferred to a chloroform-containing vessel with clean forceps, dried and placed in a plasma cleaner (100 W) for 5 min. Films of gastric tubulovesicles were obtained by drying an aqueous vesicle suspension. Placed in a flow cell (1 ml/min) for 2 h, the H^+, K^+-ATPase activity was recovered from the resuspended film [42].

Even though the immersion of films in a flow cell can be a very useful tool for the study of small conformational changes in an aqueous environment, furthermore studies to define the experimental conditions which govern the stability of the membrane assembly are needed.

In ATR-FTIR experiments under buffer flow, a sensitivity of at least one order of magnitude better than the classical techniques can be reached, as previously demonstrated by Fringeli et al. [32] for thin films, by Marrero and Rothschild [35] for thick purple membrane films, by Baenziger for thick acetylcholine receptor-containing films [43,44] and by ourselves for the gastric ATPase [45].

4.5. Protein adsorption

Adsorption of soluble proteins from an aqueous phase on a clean IRE is linear with the bulk concentration up to a concentration of 60 mg/ml and intensity of the major bands of proteins is proportional to the amount adsorbed up to 0.2 $\mu g/cm^2$ [46,47]. In our hands, working in the presence of an aqueous solution (e.g. with a Circle® cell), even with very soluble proteins, adsorption on IRE such as germanium and KRS-5 always occurs. Adsorption from an aqueous phase on the IRE is first irreversible, involving some degree of protein denaturation. Subsequent layers of adsorbed proteins can coat the IRE in which the protein structure is usually maintained [48,49]. Recently, a modelisation of the events occurring near the GeO_2 interface was obtained by molecular dynamics [50]. The process has been described in details by Oberg [51–53]. When the IRE is placed in contact with a protein solution, after some time three classes of protein can be distinguished. In a first stage of the interaction, protein molecules that come in contact with the IRE surface are free to associate in a manner dictated by the chemical nature of both the IRE surface and the protein. After they initially bind, protein molecules extent their interaction with the surface which result in significant disruption of secondary structure and changes in the amide I band shape. This process is fast and present little dependence on the bulk concentration. These adsorbed protein molecules form the first class. They remain firmly bound to the IRE after a buffer wash. The second stage begins when most of the IRE surface is covered by adsorbed protein molecules. Newly arrived protein molecules are prevented to form additional contact with the IRE surface. These protein molecules remain in a native conformation and can be flushed away by a buffer flow. These protein molecules form a second class. The third class consists in proteins which remain in the bulk of the solution. Since the ATR-FTIR technique samples preferentially the molecules close to the IRE surface, only classes 1 and 2 will contribute significantly to the spectrum. It was shown by Oberg [51–53] that the contribution of the class 1, adsorbed, proteins could be reliably estimated and subtracted from the experimental spectrum in order to yield a native protein spectrum. Even though no sensor building has been attempted by this approach, it remains a tempting possibility as it is particularly simple to prepare.

5. Chemical modification of the IREs

5.1. Silylation of the IRE

In 1979, Fringeli discovered that enzymatically active acetylcholinesterase can be covalently bound to aminosilane coating on germanium IREs by means of carbodiimide [54] after silanization by aminopropyltriethoxysilane (1% in anhydrous toluene, 1–2 h, 100 °C). This procedure was studied in more detains by Weigel and Kellner [55] but more recently, several authors found it more efficient to deposit a first layer of SiO_2. In a first step, the surface is covered with a thin layer of SiO_2 by plasma-enhanced chemical vapor deposition. The surface is first exposed to a O_2 plasma and heated to 300 °C to remove all organic contaminants. The SiO_2 film is deposited from a gaz atmosphere of SiH_4 and N_2O in the plasma oven.

Interestingly, the thickness of the layer can be monitored by the absorbance of the ν_{as}(Si–O) at 1050 cm^{-1}. Rigler et al. [2] evaluated the evanescent electric field decay as a function of the thickness of the SiO_2 layer and showed that a 30 nm thick film reduces the field intensity by less that 10%. Characterization of the surface by contact angles indicates that Ge is as good a substrate for silylation as quartz plates. Immediately after silylation, the silanol surface can be treated with a molecule such as the mercaptopropyltrimethoxysilane, providing the user with a convenient –SH group for attaching other molecules. Rigler et al. [2] suggested the binding of NTA–maleimide. After chelation of Ni^{2+} ions, His-tagged peptides or proteins can be reversibly attached. Recycling is then best obtained by washing the sensor with imidazole. The sensitivity is in the range of 10 pg/mm^2, i.e. similar to the plasmon resonance detection.

When the sensor is designed to work in aprotic solvents, another approach is possible. Poston et al. [56], instead of working with a flat surface, deposited a thin layer of colloidal silica particles onto a ZnSe IRE. The result is a high area substrate available for ATR-FTIR and a better sensitivity. The film was deposited onto the IRE by withdrawing the substrate from the sol. Upon drying, a network of siloxane and hydrogen bonds hold the network in place, leading to a porous SiO_2 layer that is stable in contact with aprotic solvents. Once the film is deposited by sol–gel synthesis, it can be modified to produce the desired chemical environment. In one interesting example, the sol used for the fabrication of silica films was prepared by an acid-catalyzed copolymerization of a one-to-one mixture of tetraethylorthosilicate (TEOS) and ethyltrimethoxysilane (ETES) in an ethanol/water medium. The molar ratio of the sol mixture components TEOS/ETES/H_2O/EtOH/HCl was 0.5:0.5:5.0:3.8:0.04. A thin film was formed on the silicon ATR crystal by dipcoating in a nitrogen atmosphere. After heating at 400 °C, porous silica films with good mechanical properties and high surface areas. The surface was then modified by octyltrichlorosilane and finally washed with toluene. After treatment, the sensor may be used in an aqueous environment [57]. Depending on the coating, the affinity for various organic molecules in solution in water can be modulated.

5.2. Au coating of the surface

The Ge IRE is coated with a 2–10 nm thick film of Au on one face by thermal evaporation at a pressure below 5×10^{-6} mbar [2]. It is necessary to deposit a first layer of Cr (0.5–1.0 nm) in order to obtain sufficient adhesion of the Au film and to produce a continuous film of Au. Failure to proceed in that way results in the formation of isolated Au particle. The space left free between the particles forms non-specific binding sites for the proteins and makes the sensor virtually useless. Instead of depositing a Cr layer, the surface can be silanized with mercaptopropyltrimethoxysilane (MTS). Alternatively, the coating can be performed with an AuPd alloy by thermal evaporation without Cr or MTS. The latter AuPd film has better wetting properties, which allows the production of thinner metal layers, which in turn improved the FTIR signal [2]. The advantage of this approach is that it can be applied to Ge, Si or ZnSe IRE.

The effect of the Au thickness on the transmittance of the IRE is large. The intensity of the sample was reported to be 10 times higher on a 2 nm Au film than on a 10 nm Au film. This dramatic change was assigned to the strong absorbance of Au [2]. On the other hand, the author realized that the absorbance is in fact higher than expected. They concluded that a surface enhancement of the absorbance due to the close proximity of the Au is taking place in agreement with the description made by Kellner et al. [58]. In this respect, no difference could be observed between Ge or ZnSe. In spite of the surface enhancement effect provided by Au, the signal to noise ratio is twice as large when compared to the silanized surface because of the lower optical throughput with Au-coated surfaces [2].

5.2.1. Indirect protein binding to Au

The most widely used strategy is to bind a thiol on the Au and keep another reactive group at the other end of the molecule. This is classical chemistry and will not be described here any further.

5.2.2. Direct protein binding to Au

In at least one example, a mutant of OmpF with a cystein introduced on a short periplasmic turn, has been shown to bind directly to gold and create a high density protein monolayer by self-assembly from the detergent solution. The protein retains its capability to bind the receptor-binding domain (R domain) of colicin N [59].

5.2.3. Thiolipid binding to Au

Reconstitution of solubilized vesicles (44 mM CHAPS) in the presence of a mixture containing a thiolipid, cholesterol and soybean lecithin (0.1:0.1:0.8, w:w:w, respectively) can be achieved by dialyzing away the CHAPS [60]. Nicotinic acetylcholine receptor membranes reconstituted with thiolipids were immobilized on Au-coated ZnSe IREs. It was found that approximately 65% of the receptors present their ligand-binding site towards the lumen of the flow cell and that at least 85% of these receptors are structurally intact. The conformation of the receptor in tethered membranes was investigated with Fourier transform infrared spectroscopy and found to be practically identical to that of receptors reconstituted in lipid vesicles. The affinity of small receptor ligands was determined in a competition assay against a monoclonal antibody directed against the ligand-binding site which yielded dissociation constants in agreement with radioligand binding assays [60].

5.3. Supported membranes on soft polymer cushions

It is most useful to be able to prepare a layer that is biocompatible between the solid support and the solution in or-

der to prevent unspecific adsorption. Sackmann and Tanaka [61] distinguish three methods for the preparation of stable polymer-membrane composite films: (1) chemical grafting of a natural polymer such as dextran or hyaluronic acid and subsequent deposition of a lipid bilayer; (2) deposition of membranes whose lipid head groups have been modified (lipopolymers), (3) deposition of soft hydrophilic or hydrophobic multilayers of rod-like molecules. In most cases, the linkage is obtained for alkyl silanes (Si, SiO_2) or alkyl mercaptanes (gold) carrying functional groups, which can be covalently coupled to the polymers. Electrochemical deposition of ultrathin films can be obtained at the anode when the polymer (e.g. polyethyleneglycol) is coupled to phenol derivatives which can be polymerized at the anode surface [61]. Even though no experiment with germanium have been reported, our experience with germanium indicates that its conductivity is probably high enough to perform the polymerization.

6. Trapping organic molecules in polymers films

One particular application of ATR-FTIR in the field of sensors is found in the use of ATR IRE coated with polymers for the analysis of environmentally significant organic compounds, including chlorinated hydrocarbon [62–65] and pesticides [66,67]. This procedure is highly sensitive as the polymers concentrates the organic molecules in agreement with a partition coefficient that favors the polymers and shields the IR evanescent wave from the water as soon at the film thickness reaches ca. 3–5 times the penetration depth. Furthermore, the diffusion rate of the organic molecules through the polymer can be monitored. As fast scanning is available (ms), the kinetic of the binding diffusion rates could be evaluated.

Acha et al. [64] described the continuous on-line monitoring of a dechlorination process by a novel attenuated total reflection-Fourier transform infrared (ATR-FTIR) sensor. This optical sensor was developed to measure non-invasively parts-per-million (ppm) concentrations of trichloroethylene (TCE), tetrachloroethylene (PCE), and carbon tetrachloride (CT) in the aqueous effluent of a fixed-bed dechlorinating bioreactor, without any prior sample preparation. The sensor was based on an ATR internal reflection element (IRE) coated with an extracting hydrophobic polymer, which prevented water molecules from interacting with the infrared (IR) radiation. The selective diffusion of chlorinated compound molecules from aqueous solution into the polymer made possible their detection by the IR beam. With the exclusion of water the detection limits were lowered, and measurements in the low ppm level became possible. The best extracting polymer was polyisobutylene (PIB) film, which afforded a detection limit of 2, 3, and 2.5 ppm for TCE, PCE, and CT, respectively. Values of the enrichment factors between the polymer coating and the water matrix of these chloro-organics were determined experimentally and were compared individually with predictions obtained from the slopes of absorbance/concentration curves for the three analytes.

Murphy et al. [68] used Teflon AF2400, a highly amorphous and robust polymer for the enrichment membrane and various environmentally significant chlorinated hydrocarbon and alcohol species selected as analytes. Analyses were performed on aqueous solutions running in continuous flow configuration. Diffusion coefficients, calculated through regression of experimental data with simulated Fickian diffusion curves, were employed as the primary indicator of diffusion behavior. Penetrant size and shape were both demonstrated to exhibit a substantial impact upon diffusion behavior. In another example, the diffusion of drugs through a 0.3 mm thick silicone membrane was investigated [69]. In such a case, the diffusion process is relevant of the penetration of the drug through natural barriers such as skin.

6.1. Spectral processing

In general, the sensor will have different channels, one of them being used as a reference. Even in that situation, three problems remain:

1. Water vapor content may vary in the sample compartment between the recording of the sample and of the reference. This is usually insignificant but when working with monomolecular films, the intensity changes can be as low as μAU and vapor contribution might require correction. Separation of atmospheric water contribution from protein bands is in principle simple because of the huge difference of intrinsic bandwidth. However, when spectra are recorded at 4 or even 8 cm^{-1}, part of this advantage is lost. Working at reasonably high resolution provides the spectroscopist with a good test to differentiate the contribution of the condensed phase from the contribution of the atmospheric H_2O bands as demonstrated earlier [70]. The correct subtraction coefficient could be defined within 1.4% for 0.5 cm^{-1} resolution spectra but only within 60% for 4 cm^{-1} resolution spectra [70]. CO_2 absorbance may also vary in the course of an experiment but the CO_2 contribution is present only in the 2400–2300 cm^{-1} region of the spectrum, a frequency domain with no absorbance from the biological molecules. In turn, absorbance from CO_2 is never a problem.
2. In the course of hours, baseline shit may occur. This is generally not a problem as a linear baseline is generally fitted between several points of the spectrum and subtracted.
3. Binding of any molecule on the sensor surface also implies a displacement of some other molecules, most often water. This displacement results in a negative contribution assigned to the removal of some water from the evanescent field. This effect is difficult to correct as the displaced water is largely bound water characterized by an IR spectrum different from the bulk water.

4. The method is very sensitive to swelling and shrinking of the layers attached to the IRE as this produces a significant displacement of the bound materials along the *z*-axis (Fig. 1). In turn, the overall intensity of the contribution of the layer molecules to the film varies. We found that the problem is largely alleviate if care is taken to maintain a constant ionic strength in the course of the measurements.
5. Signal-to-noise level is in general excellent in infrared spectroscopy. In a recent paper [71], Scheirlinckx et al. showed that for a single IR difference spectrum, the mean standard deviation over 2800–2200 cm^{-1} region reached 7.4×10^{-6} A.U. A mean spectrum of 10 difference spectra had a typical standard deviation of 2.0×10^{-6} A.U. over the same region. This improvement was expected as noise decreases as the square root of the number of experiments. In this case, the measurements are so reproducible that it becomes possible to visualize a conformational change affecting less than six residues in a large glycosylated and membrane-embedded protein. This realistic situation takes into account the film stability, the ionic strength effects and the effect of the ligands on the spectrum of water.

7. Future prospects

We have described here the first attempts to use ATR-FTIR to prepare sensors. So far, ATR-FTIR is not yet widely used for sensor building. The technique is promising but the actual achievements are still limited. It is therefore not possible to guess which of the methods described here is going to develop. Yet, it appears that some kind of covalent binding between the IRE and the "receptors" is essential to make a device stable in the long run. Langmuir–Blodgett or multilayers might not be stable enough in stringent working conditions. Casting a metal layer (mainly gold) is not a perfect solution as it cuts part of the light, thereby increasing the noise level. It appears that direct binding on the IRE by a covalent linkage might turn out to become the best solution. More work might be needed to improve the efficiency and the control of the chemistry on the most interesting IRE such as germanium.

One major advantage of future sensors will be they capability to measure multiple parameters using a combination of electrical and optical techniques. Both electrical measurements and visible spectroscopy have been associated with FTIR spectroscopy in the past [72–78]. Designing of ATR cells able to associated several measurement types is a promising issue for a near future.

The other way of progress is in the design of smaller and more sensitive sensors which ultimately will result in the manufacturing of protein chips. Recently, Plunkett et al. [79] succeeded in making miniature supported planar waveguides with the goal of observing structural changes in transmembrane proteins functioning in vivo in single cells. Spectra of subpicomolar concentrations will probably be obtainable in a near future. High signal-to-noise Fourier transform infrared (FTIR) spectra of the 5-hydroxytryptamine (serotonin) receptor (5-HT3R) and the nicotinic acetylcholine receptor (nAChR) were obtained by microscope FTIR spectroscopy using micrometer-sized, fully hydrated protein films. Because this novel procedure requires only nanogram quantities of membrane proteins, which is four to five orders of magnitude less than the amount of protein typically used for conventional FTIR spectroscopy, it opens the possibility to access the structure and dynamics of many important mammalian receptor proteins [80]. On the other hand, a methodology for the deposition of extremely small volumes (attoliters (10^{-18} l)) has been designed by Stamou et al. [81].

Acknowledgments

E.G. is Director of Research and C.V. Post-doctoral researcher with the "*National Fund for Scientific Research*", Belgium. We thank the "Communauté Française de Belgique—Actions de Recherches Concertées" for financial support.

References

[1] E. Goormaghtigh, V. Raussens, J.M. Ruysschaert, Biochim. Biophys. Acta 1422 (1999) 105–185.
[2] P. Rigler, W.P. Ulrich, P. Hoffmann, M. Mayer, H. Vogel, Chem. Phys. Chem. 4 (2003) 268–275.
[3] M.J. Citra, P.H. Axelsen, Biophys. J. 71 (1996) 1796–1805.
[4] G. Müller, K. Abraham, M. Schaldach, Appl. Opt. 20 (1981) 1182–1190.
[5] U.P. Fringeli, in: F.M. Mirabella (Ed.), Internal Reflection Spectroscopy, Marcel Dekker Inc, 1992.
[6] V. Grimard, C. Vigano, A. Margolles, R. Wattiez, H.W. van-Veen, W.N. Konings, J.M. Ruysschaert, E. Goormaghtigh, Biochemistry 40 (2001) 11876–11886.
[7] R.I. Saba, E. Goormaghtigh, J.M. Ruysschaert, A. Herchuelz, Biochemistry 40 (2001) 3324–3332.
[8] M. Hollecker, M. Vincent, J. Gallay, J.M. Ruysschaert, E. Goormaghtigh, Biochemistry 41 (2002) 15267–15276.
[9] C. Vigano, V. Grimard, A. Margolles, E. Goormaghtigh, H.W. van Veen, W.N. Konings, J.M. Ruysschaert, FEBS Lett. 530 (2002) 197–203.
[10] K.A. Oberg, J.M. Ruysschaert, E. Goormaghtigh, Prot. Sci. 12 (2003) 2015–2031.
[11] N.J. Harrick, Interscience Publishers, New York, 1967.
[12] S. Simhony, A. Katzir, E.M. Kosower, Anal. Chem. 60 (1988) 1908–1910.
[13] S. Simhony, I. Schnitzer, A. Katzir, E.M. Kosower, J. Appl. Phys. 64 (1988) 3732–3734.
[14] S. Simhony, E.M. Kosower, A. Katzir, Biochem. Biophys. Res. Commun. 142 (1987) 1059–1063.
[15] S. Simhony, E.M. Kosower, A. Katzir, Appl. Phys. Lett. 49 (1986) 253–254.
[16] U.P. Fringeli, J. Membr. Biol. 54 (1980) 203–212.
[17] U.P. Fringeli, Chimia 46 (1992) 200–214.
[18] K.B. Blodgett, I. Langmuir, Phys. Rev. 51 (1937) 964–982.
[19] H. Khun, B. Möbius, H. Bücher, in: A. Weisenberger, B. Rossiter (Eds.), Techniques of Chemistry, Wiley, New York.
[20] L. Silvestro, P.H. Axelsen, Chem. Phys. Lipids 96 (1998) 69–80.
[21] L.K. Tamm, C. Bohm, J. Yang, Z.F. Shao, J. Hwang, M. Edidin, E. Betzig, Thin Solid Films 285 (1996) 813–816.

[22] E. Okamura, J. Umemura, T. Takenaka, Biochim. Biophys. Acta 812 (1985) 139–146.
[23] F. Kopp, U.P. Fringeli, K. Muhlethaler, H.H. Günthard, Biophys. Struct. Mech. 1 (1975) 75–96.
[24] F. Kopp, U.P. Fringeli, H.H. Gunthard, Z. Naturfosch. 30c (1975) 711–717.
[25] F.R. Rana, B.W. Widayati, B.W. Gregory, R.A. Dluhy, Appl. Spectrosc. 48 (1994).
[26] R.A. Dluhy, in: D.G. Cameron (Ed.), Proceedings of the Seventh International Conference on Fourier Transform Spectroscopy, Proceeding on the SPIE, Bellingham, WA, 1989.
[27] R.A. Dluhy, S.A. Stephens, W.S. Widayati, A.D. Williams, Spectrochim. Acta Part A 51 (1998) 1413–1447.
[28] D.G. Cornell, R.A. Dluhy, M.S. Briggs, C.J. McKnight, L.M. Gierasch, Biochemistry 28 (1989) 2789–2797.
[29] M.S. Briggs, D.G. Cornell, R.A. Dluhy, L.M. Gierasch, Science 233 (1986) 206–208.
[30] M.S. Briggs, L.M. Gierasch, Adv. Protein Chem. 38 (1986) 109–180.
[31] M. Boncheva, H. Vogel, Biophys. J. 73 (1997) 1056–1072.
[32] U.P. Fringeli, H.J. Apell, M. Fringeli, P. Lauger, Biochim. Biophys. Acta 984 (1989) 301–312.
[33] S. Frey, L.K. Tamm, Biophys. J. 60 (1991) 922–930.
[34] L.K. Tamm, S.A. Tatulian, Biochemistry 32 (1993) 7720–7726.
[35] H. Marrero, K.J. Rothschild, Biophys. J. 52 (1987) 629–635.
[36] J.E. Baenziger, K.W. Miller, K.J. Rothschild, Biochemistry 32 (1993) 5448–5454.
[37] J.E. Baenziger, N. Méthot, J. Biol. Chem. 270 (1995) 29129–29137.
[38] J.E. Baenziger, J.P. Chew, Biochemistry 36 (1997) 3617–3624.
[39] N. Méthot, M.P. McCarthy, J.E. Baenziger, Biochemistry 33 (1994) 7709–7717.
[40] N. Méthot, C.N. Demers, J.E. Baenziger, Biochemistry 34 (1995) 15142–15149.
[41] S.E. Ryan, C.N. Demers, J.P. Chew, J.E. Baenziger, J. Biol. Chem. 271 (1996) 24590–24597.
[42] V. Raussens, J.M. Ruysschaert, E. Goormaghtigh, J. Biol. Chem. 272 (1997) 262–270.
[43] J.E. Baenziger, K.W. Miller, K.J. Rothschild, Biophys. J. 61 (1992) 983–992.
[44] J.E. Baenziger, K.W. Miller, M.P. McCarthy, K.J. Rothschild, Biophys. J. 62 (1992) 64–66.
[45] D. Vanderstricht, V. Raussens, K.A. Oberg, J.M. Ruysschaert, E. Goormaghtigh, Eur. J. Biochem. 268 (2001) 2873–2880.
[46] D.J. Fink, T.B. Hutson, K.K. Chittur, R.M. Gendreau, Anal. Biochem. 165 (1987) 147–154.
[47] D.J. Fink, R.M. Gendreau, Anal. Biochem. 139 (1984) 140–148.
[48] R.J. Jacobsen, F.M. Wasacz, in: J.L. Brash, T.A. Horbett (Eds.), Proteins at Interfaces, American Chemical Society Books, Washington, DC, 1987.
[49] R.J. Jacobsen, F.M. Wasacz, J.W. Brasch, K.B. Smith, Biopolymers 25 (1986) 639–654.
[50] A.M. Bujnowski, W.G. Pitt, J. Biomater. Sci. Polym. 13 (2002) 885–906.
[51] K.A. Oberg, Dissertation thesis, 1994, pp. 1–217.
[52] K.A. Oberg, A.L. Fink, Anal. Biochem. 256 (1998) 92–106.
[53] K.A. Oberg, A.L. Fink, Techniques in Protein Chemistry VI, 1995.
[54] P. Hofer, U.P. Fringeli, Biophys. Struct. Mech. 6 (1979) 67–80.
[55] C. Weigel, R. Kellner, Fresenius Zeitschrift fur Analytische Chemie 335 (1989) 663–668.
[56] P.E. Poston, D. Rivera, R. Uibel, J.M. Harris, Appl. Spectrosc. 52 (1998) 1391–1398.
[57] L. Han, T.M. Niemczyk, Y.F. Lu, G.P. Lopez, Appl. Spectrosc. 52 (1998) 119–122.
[58] R. Kellner, B. Mizaikoff, M. Jakusch, H.D. Wanzenbock, N. Weissenbacher, Appl. Spectrosc. 51 (1997) 495–503.
[59] S. Terrettaz, W.P. Ulrich, H. Vogel, Q. Hong, L.G. Dover, J.H. Lakey, Prot. Sci. 11 (2002) 1917–1925.
[60] A. Sevin-Landais, P. Rigler, S. Tzartos, F. Hucho, R. Hovius, H. Vogel, Biophys. Chem. 85 (2000) 141–152.
[61] E. Sackmann, M. Tanaka, Trends Biotechnol. 18 (2000) 58–64.
[62] V. Acha, M. Meurens, H. Naveau, D. Dochain, G. Bastin, S.N. Agathos, Water Sci. Technol. 40 (1999) 33–40.
[63] V. Acha, M. Meurens, H. Naveau, S.N. Agathos, Water Sci. Technol. 40 (1999) 41–47.
[64] V. Acha, M. Meurens, H. Naveau, S.N. Agathos, Biotechnol. Bioeng. 68 (2000) 473–487.
[65] R. Gobel, R. Krska, R. Kellner, R.W. Seitz, S.A. Tomellini, Appl. Spectrosc. 48 (1994) 678–683.
[66] F. Regan, M. Meaney, J.G. Vos, B.D. MacCraith, J.E. Walsh, Anal. Chim. Acta 334 (1996) 85–92.
[67] J.E. Walsh, B.D. MacCraith, M. Meaney, J.G. Vos, F. Regan, A. Lancia, S. Artjushenko, Analyst 121 (1996) 789–792.
[68] B. Murphy, P. Kirwan, P. McLaughlin, Anal. Bioanal. Chem. 377 (2003) 195–202.
[69] K. Moser, K. Kriwet, C. Froehlich, A. Naik, Y.N. Kalia, R.H. Guy, J. Pharm. Sci. 90 (2001) 607–616.
[70] E. Goormaghtigh, J.M. Ruysschaert, Spectrochim. Acta 50A (1994) 2137–2144.
[71] F. Scheirlinckx, V. Raussens, J.M. Ruysschaert, E. Goormaghtigh, Biochem. J. 382 (2004) 121–129.
[72] M. Ritter, O. Anderka, B. Ludwig, W. Mantele, P. Hellwig, Biochemistry 42 (2003) 12391–12399.
[73] P. Hellwig, B. Rost, W. Mantele, Spectrochim. Acta Part A: Mol. Biomol. Spectrosc. 57 (2001) 1123–1131.
[74] E. Nabedryk, J. Breton, R. Hienerwadel, C. Fogel, W. Mantele, M.L. Paddock, M.Y. Okamura, Biochemistry 34 (1995) 14722–14732.
[75] E. Nabedryk, J. Breton, R. Hienerwadel, W. Mantele, M.L. Paddock, S.H. Rongey, G. Feher, M.Y. Okamura, Biophys. J. 64 (1993) 214.
[76] A. Remy, K. Gerwert, Nat. Struct. Biol. 10 (2003) 637–644.
[77] R. Brudler, R. Rammelsberg, T.T. Woo, E.D. Getzoff, K. Gerwert, Nat. Struct. Biol. 8 (2001) 265–270.
[78] D. Moss, E. Nabedryk, J. Breton, W. Mantele, Eur. J. Biochem. 187 (1990) 565–572.
[79] S.E. Plunkett, R.E. Jonas, M.S. Braiman, Biophys. J. 73 (1997) 2235–2240.
[80] P. Rigler, W.P. Ulrich, R. Hovius, E. Ilegems, H. Pick, H. Vogel, Biochemistry 47 (2003) 14017–14022.
[81] D. Stamou, C. Duschl, E. Delamarche, H. Vogel, Angew. Chem. Int. 42 (2003) 5580–5583.